

Supporting Information

Temperature-dependent Ultraviolet Photoluminescence in Hierarchical Zn, ZnO and ZnO/Zn Nanostructures

Han-Sheng Chou,¹ Kai-Di Yang,² Sheng-Hong Xiao,¹ Ranjit A. Patil,^{1,*} Chien-Chih Lai,¹ Wang-Chi Vincent Yeh,¹ Ching-Hwa Ho,² Yung Liou,³ and Yuan-Ron Ma^{1,*}

¹*Department of Physics, National Dong Hwa University, Hualien 97401, Taiwan*

²*Graduate Institute of Applied Science & Technology and Department of Electronic & Computer Engineering, National Taiwan University of Science and Technology, Taipei 106, Taiwan*

³*Institute of Physics, Academia Sinica, Taipei 11529, Taiwan*

The supporting information contains the room-temperature and ambient-air PL emissions of the 2D-hierarchical ZnO/Zn nanostructures (Fig. S1, after annealing of the 2D Zn nanosheets at 400 and 550 °C), variable-power PL emissions at various temperatures (Fig. S2), normalized-intensity mappings at various temperatures (Fig. S3), maximum PL peak evolution with elevated laser power at various temperatures, and CIE 1931 (X,Y) tristimulus values of the PL spectra of the 2D-hierarchical ZnO nanostructure, 2D Zn nanosheets and 2D-hierarchical Zn/ZnO nanostructures measured at various temperatures.

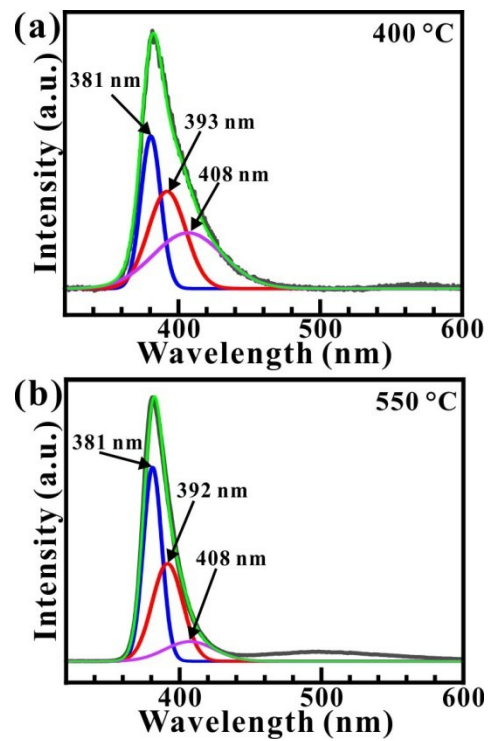


Figure S1. PL emissions. (a) and (b) Room-temperature and ambient-air PL spectra of the 2D-hierarchical ZnO/Zn nanostructures (after annealing 2D Zn nanosheets at 400 and 550 °C).

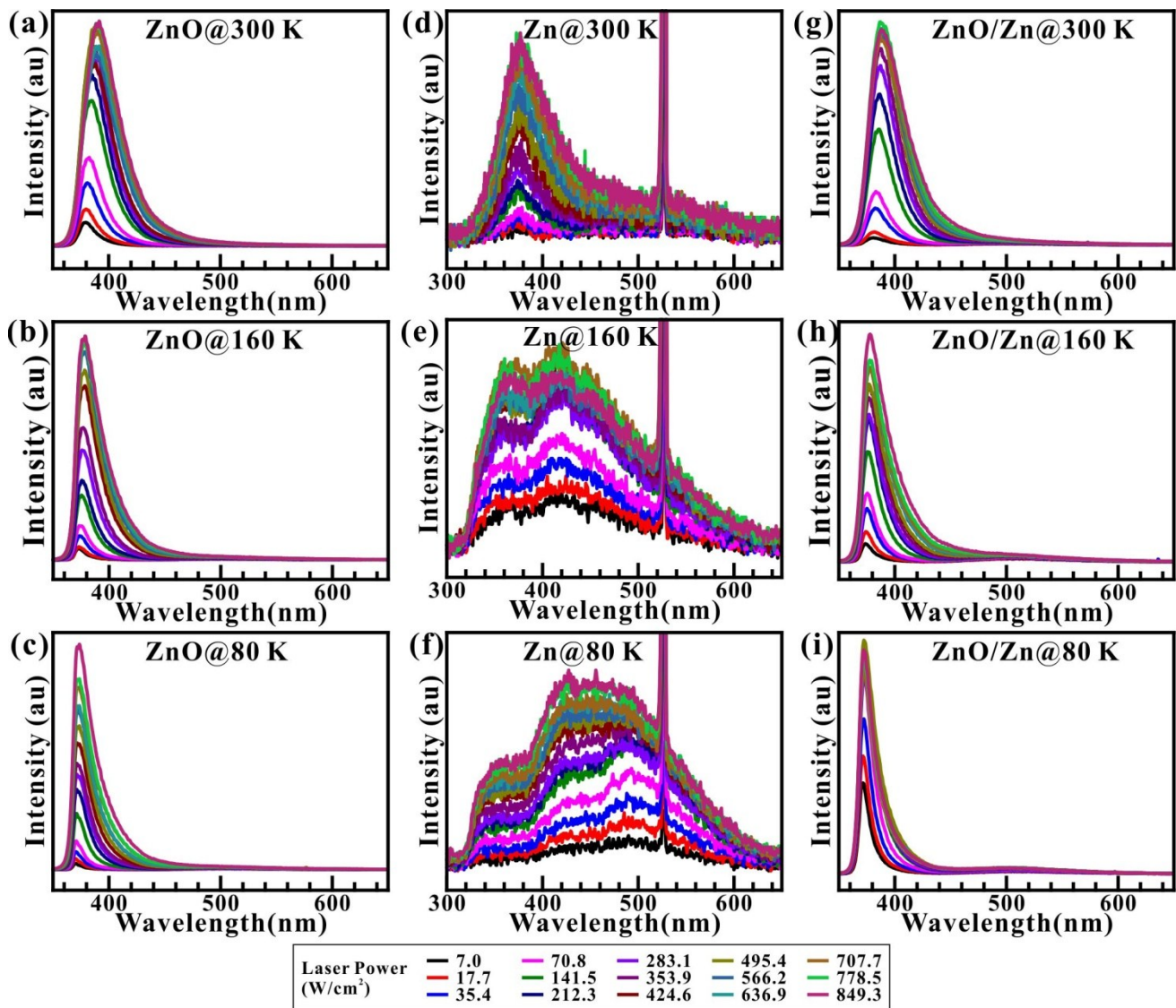


Figure S2. Variable-power PL emissions at various powers. (a)-(c) Variable-power PL spectra of the 2D-hierarchical ZnO nanostructures at 300, 160, and 80 K, respectively. (d)-(f) Variable-power PL spectra of the as-synthesized Zn nanosheets at 300, 160, and 80 K, respectively. (g)-(i) Variable-power PL spectra of the 2D-hierarchical ZnO/Zn nanostructures at 300, 160, and 80 K, respectively. Note that the power of the incident laser is easily tuned to be the values as listed in the box above.

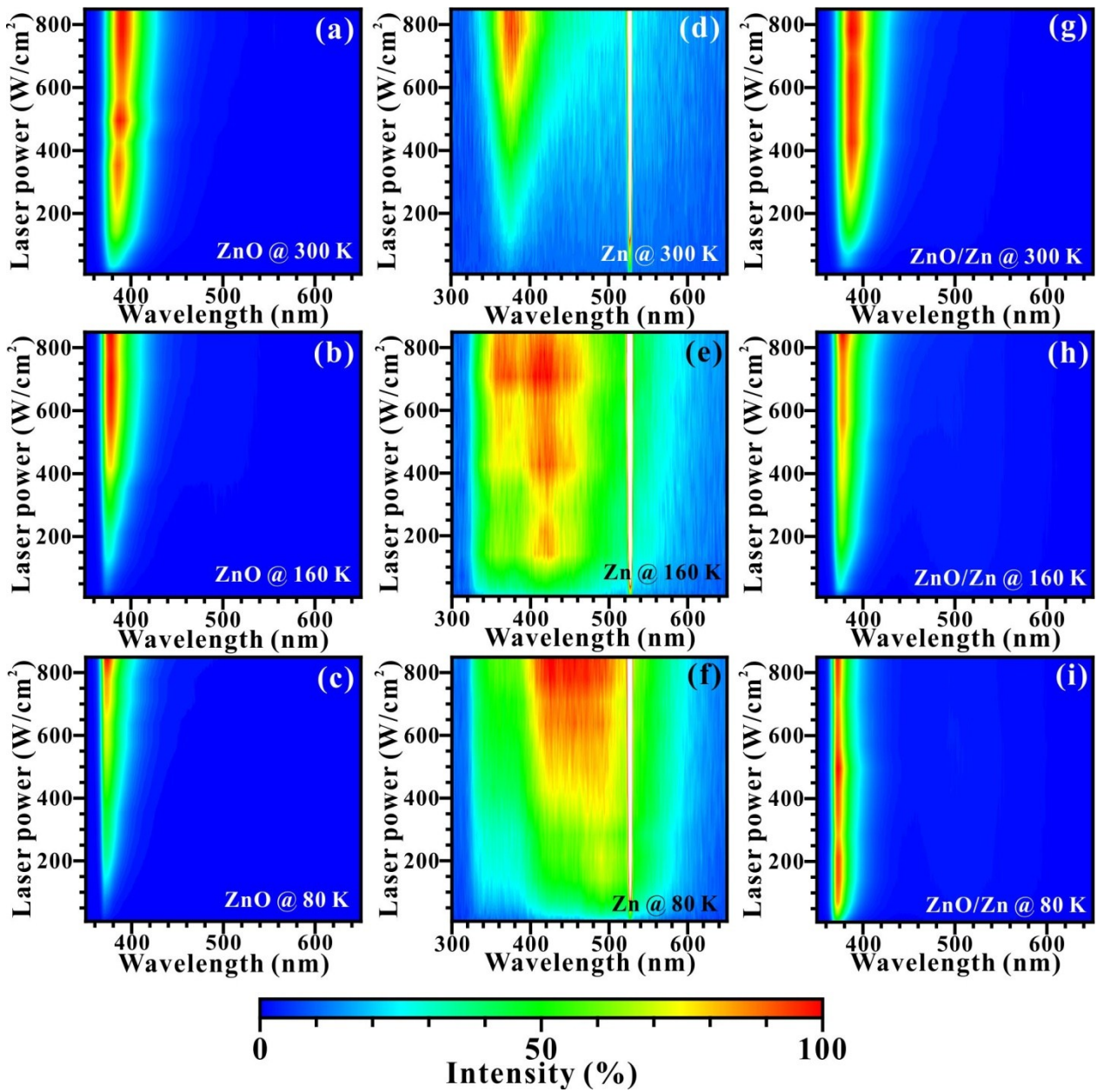


Figure S3. Normalized-intensity mappings at various powers. According to the variable-power PL results in Fig. S2, the spectra of the variable-power PL emissions can be converted into the normalized-intensity mappings of variable-power PL emissions at varying low temperatures. (a)-(c) Variable-power PL mappings of the 2D-hierarchical ZnO nanostructures at 300, 160, and 80 K, respectively. (d)-(f) Variable-power PL mappings of the as-synthesized Zn nanosheets at 300, 160, and 80 K, respectively. (g)-(i) Variable-power PL mappings of the 2D-hierarchical ZnO/Zn nanostructures at 300, 160, and 80 K, respectively.

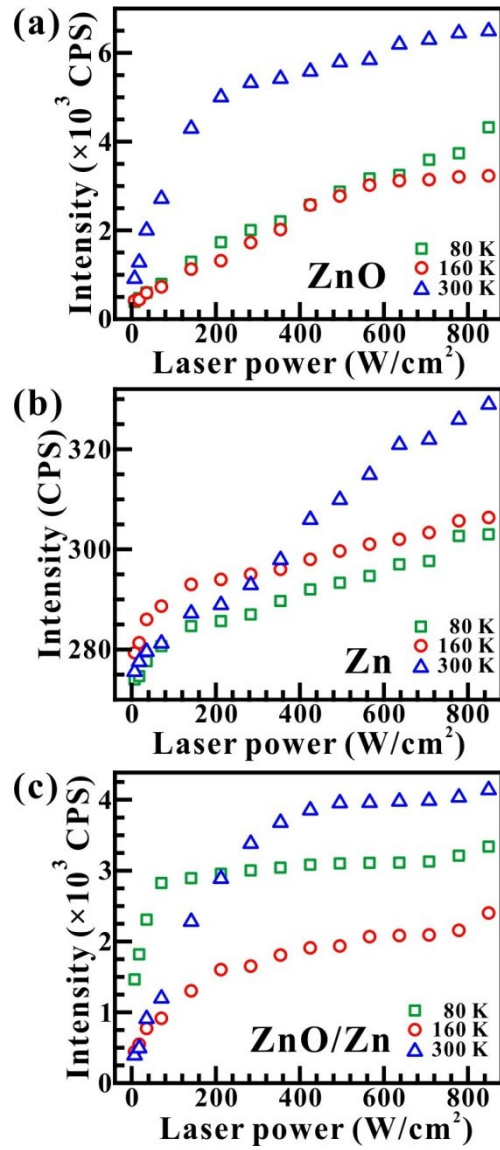


Figure S4. Maximum PL peak evolution with elevated laser power at various temperatures. (a)-(c) Linear graphs of PL intensities (I_T) as functions of laser power at 80, 160, 300 K, respectively, for the (a) ZnO nanostructures, (b) Zn nanosheets, and (c) ZnO/Zn nanostructures. A linear enhancement in PL intensity in ZnO/Zn and ZnO holds only for low excitation power as shown in Fig. S4(a) and S4(c) however, fails at high excitation power. This inconsistent PL enhancement is attributed to the creations of bound excitons due to high excitations power. Therefore, PL intensity associated with bound excitons saturate at high excitation power due to enhancement non-radiative recombinations via bound excitons^[S1]. At high power excitations, the creation of bound excitons is higher due to the neutralization of donors/acceptors by photoexcited carriers^[S2].

- S1. S. Tongay, J. Suh, C. Ataca, W. Fan, A. Luce, J. S. Kang, J. Liu, C. Ko, R. Raghunathanan, J. Zhou, F. Ogletree, J. Li, J. C. Grossman, J. Wu, Sci. Rep. 3 (2013) 2657
- S2. T. Schmidt, K. Lischka, W. Zulehner, Phys. Rev. B 45 (1992) 8989–8994.

Table S1. CIE 1931 (X,Y) tristimulus values of the PL spectra of the 2D-hierarchical ZnO nanostructure, 2D Zn nanosheets and 2D-hierarchical Zn/ZnO nanostructures measured at various temperatures.

Temperature (K)	ZnO		Zn		Zn/ZnO	
	X	Y	X	Y	X	Y
80	0.13177	0.30933	0.19753	0.11789	0.13474	0.23829
100	0.12518	0.34269	0.15849	0.0854	0.13596	0.24208
120	0.12261	0.36167	0.12992	0.07379	0.1349	0.22886
140	0.12062	0.37926	0.11341	0.06667	0.1324	0.26262
160	0.11455	0.40874	0.09758	0.06453	0.13176	0.25981
180	0.11394	0.42213	0.089	0.0478	0.1307	0.27393
200	0.11213	0.43561	0.07991	0.04503	0.12998	0.28109
220	0.12425	0.34128	0.07034	0.05133	0.13083	0.2657
240	0.12479	0.34347	0.0642	0.04384	0.13263	0.26385
260	0.12356	0.35007	0.05899	0.04545	0.13155	0.27222
280	0.12204	0.36337	0.05403	0.04662	0.13146	0.27946
300	0.12103	0.37116	0.05098	0.03901	0.1307	0.2781